10TH INTERNATIONAL SYMPOSIUM ON PARTICLE IMAGE VELOCIMETRY – PIV13
Delft, The Netherlands, July 2-4, 2013

Evaluation of pool boiling heat transfer over micro-structured surfaces by combining high-speed visualization and PIV measurements

E. Teodori, A. S. Moita[1*], E. Teodori[1] and A. L. N. Moreira[1]

[1] IN+ - Instituto Superior Técnico, TU Lisbon, Lisbon, Portugal
corresponding author: anamoita@dem.ist.utl.pt

ABSTRACT

The present work introduces an alternative approach which combines heat transfer measurements, high speed visualization and PIV to infer on the effect of surface micro-structuring in the various heat transfer parcels.
The PIV provides particularly interesting information on the bubbles vertical velocity, allowing to infer how the micro-structures affect the bulk induced flow. The micro-patterns are composed by arrays of cavities with fixed shape and depth, only varying the distance between cavities, *S*.
The results confirm the importance of enhancing the pool boiling performance, by promoting the increase of the bubble frequency and active nucleation sites density with micro-patterned surfaces. The role of the patterns is different, depending on the properties of the fluids. Hence, for liquids with very high latent heat of evaporation and surface tension, the parcel of heat transfer related to the phase change is very important. Based on the force balance on the departing bubbles, it is evident that in this case the micro-patterns will mainly affect the bubble coalescence, which may lead to steep deterioration of the heat transfer coefficient. On the other hand, for liquids with lower thermal properties (and lower surface tension) the micro-patterns play an important role in increasing and stabilizing the vertical velocity of the bubbles, thus favoring a very efficient boiling performance, with high boiling frequencies and large active nucleation sites density. This role of the micro-patterned surfaces is well captured by the representation proposed here, which relates the heat transfer coefficient with the distance between micro-patterns *S*, made dimensionless by the characteristic dimension ($Lc=(\sigma_{lv}/(\rho_l-\rho_v))^{1/2}$). This representation actually shows the best performance of the HFE7000 in comparison to that of ethanol, when the micro-patterned surfaces are used, despite the lower thermal properties of HFE7000. This trend was confirmed experimentally in our measurements.

INTRODUCTION

Most of the studies addressing enhanced surfaces, often modified by changing surface topography, make use of a trial and error approach, to improve the heat transfer coefficient and increase the Critical Heat Flux (e.g. [1]). Although valuable outcomes were obtained from such studies, this may not be the most effective approach given the lack of universality of the empirical correlations devised by this approach, as recently shown by McHale and Garimella [2]. While surface wettability mainly plays a role on the onset of boiling and on keeping the nucleation stable (through contact angle hysteresis), so that it affects CHF [3] surface topography promotes the increase of active nucleation sites density, but also affects significantly the interaction mechanisms (*e.g.* [4]). In [4] one has explored in detail the effect of surface topography on bubble dynamics and suggested a relation linking the distance between micro-cavities and the heat transfer coefficient. Basically, one can determine an optimum distance which maximizes the heat transfer coefficient *h* by triggering bubble growth. Further decreasing that distance, bubble coalescence near the surface will be excessively strong causing a steep deterioration of *h*. The work performed in [4] produced guiding results, which should be confirmed for a wider range of refrigerants. Also, given the considerably high latent heat of evaporation of the liquids used in [4], the relations devised are mostly related to the heat transfer parcel associated to the latent heat. However, there are other two parcels involved in the pool boiling heat transfer, namely the natural convection and the bulk convection (induced by bubble growth and motion) [5] whose relative importance is not clearly accessed.

In line with this, the present work proceeds with the analysis suggested in [4] over a wider range of liquids to infer on the relative importance of the various pool boiling heat transfer parcels. The experimental approach combines heat transfer measurements, high speed visualization and PIV to infer on the effect of surface micro-structuring in the various heat transfer parcels.

MATERIALS AND METHODOLOGY

Pool boiling is investigated for various liquids, namely the dielectric fluid HFE 7000, ethanol and water. These fluids were selected since they have a gradual decrease in the values of surface tension and of the relevant thermal properties such as the thermal conductivity, the heat capacity and the latent heat of evaporation, as shown in Table 1.

Table 1 Thermophysical properties of the liquids used in the present study, taken at saturation, at 1.013×10^5Pa.

Property	Ethanol	Water	HFE7000
T_{sat} [°C]	78.4	100	34
ρ_l [kg/m^3]	736.4	957.8	1374.7
ρ_v [kg/m^3]	1.647	0.5956	4.01
μ_l [mN m/s^2]	0.448	0.279	0.3437
C_{pl} [J/kgK]	3185	4217	1352.5
k_l [W/mK]	0.165	0.68	0.07
h_{fg} [kJ/kg]	849.9	2257	142
σ_{lv} [N/m]x10^3	17	58	12.4

Heat flux and heat transfer coefficients are determined for the various liquid/surface pairs. Afterwards, they are related to the bubble dynamics. This characterization is made by combining high-speed visualization with PIV measurements.

The micro-cavities are squares with fixed size length a=52 µm and fixed depth h_R=20µm. The distance between the centers of the cavities S is mainly our optimization variable, ranging between 300µm<S<1200µm. The parameters characterizing the micro-patterns are schematically defined in Figure 1, together with a photo of a sample.

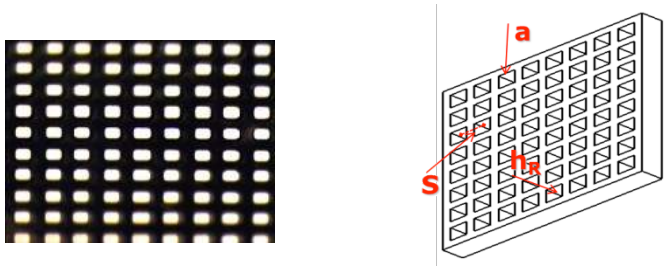

a) **b)**

Figure 1 a) Identification of the main parameters quantifying the micro-patterns. **b)** Sample of a pattern with square cavities.

Heat flux and heat transfer coefficients are determined for the various liquid/surface pairs. Afterwards, they are related to the bubble dynamics. This characterization is made by combining high-speed visualization with PIV measurements.

The patterns are custom made from silicon wafers combining wet etching with plasma etching and the roughness profiles measured using a profile meter with a precision of ±100Angstroms. Table 2 depicts the main topographical characteristics of the surfaces used in this study. The Table includes the average values of the static contact angles, which were measured as described in [6]. The contact angles obtained with ethanol and HFE7000 in contact with all the surfaces are close to zero.

Table 2 Main range of the topographical characteristics of the micro-patterned surfaces. θ is the average static contact angle measured with water at room temperature. θ≅0º for all the surfaces in contact with ethanol and HFE7000.

Material	**Reference**	***a*** **[µm]**	***h_R*** **[µm]**	***S*** **[µm]**	***θ*** **[º]**
Silicon Wafer	Smooth	≈ 0	≈ 0	≈ 0	86.0
	C1	52	20	304	90.0
	C2	52	20	400	91.5
	C3	52	20	464	71.5
	C4	52	20	626	86.5
	C5	52	20	700	95.0
	C6	52	20	800	60.5
	C7	52	20	1200	66.3

HEAT TRANSFER MEASUREMENTS

The boiling curves are presented for each liquid and each heating surface by varying the imposed heat flux in steps of 15W/cm^2. Each curve is obtained from the average of seven experiments. The liquid is degassed before each experiment by maintaining it in the pool at 20°C above the saturation temperature and the experimental procedure is started, for each heat flux, only after the system has reached thermal equilibrium, i.e. when the temperature oscillation is smaller than ±0.5 °C.

Experiments are conducted to obtain average boiling curves by both increasing and decreasing the heat flux, to infer on hysteresis effects, as also pointed by Mohamed and Bostanci [7]. The temperature measurements have an uncertainty of ±1°C. The relative error associated with the determination of the heat transfer is 5%.

IMAGE ANALYSIS OF BUBBLE DYNAMICS

Following an approach similar to that presented in many works reported in the literature, the parameters selected here to characterize bubble nucleation are the bubble departure diameter, the bubble departure frequency and the active nucleation sites density. This characterization is based on high-speed visualization and image post-processing. The images are recorded with a frame rate of 2200fps. For the optical configuration used here, the spatial resolution is 9.346μm/pixel.

The bubble departure diameter is measured for each test condition from 300 to 1060 frames. For each image a mean value is averaged from 5-16 measurements for every nucleation site that is identified in the frame.

At higher heat fluxes, the various interaction mechanisms, which will be discussed in the following section, may alter significantly the value of the departure diameter, especially when horizontal coalescence occurs. Therefore, in those cases, the measured diameters are a mean value taken from the averaged diameters, which are evaluated after the occurrence of such events close to the wall.

The error associated to the measurements of the bubble departure diameter is ±9.346 μm.

The bubble departure frequency is estimated by determining the time elapsed between apparent departure events, which are counted for a defined interval of time. The departure frequency is assessed, for each test condition, for at least five nucleation sites, which are evaluated based on extensive image post-processing of 300 to 1060 frames. The final value of the bubble departure frequency is the average between the frequencies of each nucleation site. The uncertainty associated to these measurements is ±1 fps.

Finally, the evaluation of the active nucleation sites density must be done by visual inspection of the frames, which introduces an uncertainty associated to the subjective criterion of the observer. To lessen this uncertainty, at least ten frames are chosen, at different times during the single experiment. The final values of the active nucleation site density are an average of the ten evaluated values.

PIV MEASUREMENTS

Several studies in the literature confirm the potential of using PIV to measure bubble velocity inside a flowing fluid, as for example reported by [8] and [9]. However, the results obtained from this technique are very sensitive to the characteristics of the flow and to the parameters used during the visualization and the post-processing of the images (*e.g.* [9]). In the present work, the main focus is to measure the velocity of the bubbles, so seeding was not used, but instead the bubbles are followed, as suggested by [9]. Bubbles diameter is in the range of 500-800 μm, measured by image post-processing. These dimensions and the low characteristic velocities of the bubbles (1-10 cm/s) require a careful analysis of all the parameters which have to be selected in the PIV configuration. The PIV system uses a CCD camera Kodak Megaplus, Model 1.0, with an image resolution of 1018x1008 pixel^2. The bubbles are illuminated via a dual Nd:YAG Litron laser. The PIV set-up is shown in Figure 2, together with and the coordinate system considered in the measurements.

The time delay between laser pulses is varied ($1<\Delta t<8$ms) depending on the imposed heat flux: the time between pulses is smaller for higher imposed heat fluxes. Furthermore, the interrogation area and the overlap are also varied for the various imposed heat flux conditions, in an optimization process, to assure that the chosen values are adequate to obtain accurate measurements. Hence, the selected interrogation area was varied between 16 and 64 pixels (1pixel/58μm) to assure that at least five bubbles are inside. An overlap of 50% is chosen by analyzing two consecutive frames and evaluating the average displacement of the bubbles. The most appropriate approach for this kind of flow is using a recursive cross correlation or the average correlation algorithms (*e.g.* [9]). In the present work, after analyzing extensively both approaches, the cross correlation was considered to be the most appropriate. The measurements performed using PIV are compared with extensive image post-processing, within quite good agreement. The PIV data were processed with the software Flow manager 4.2.

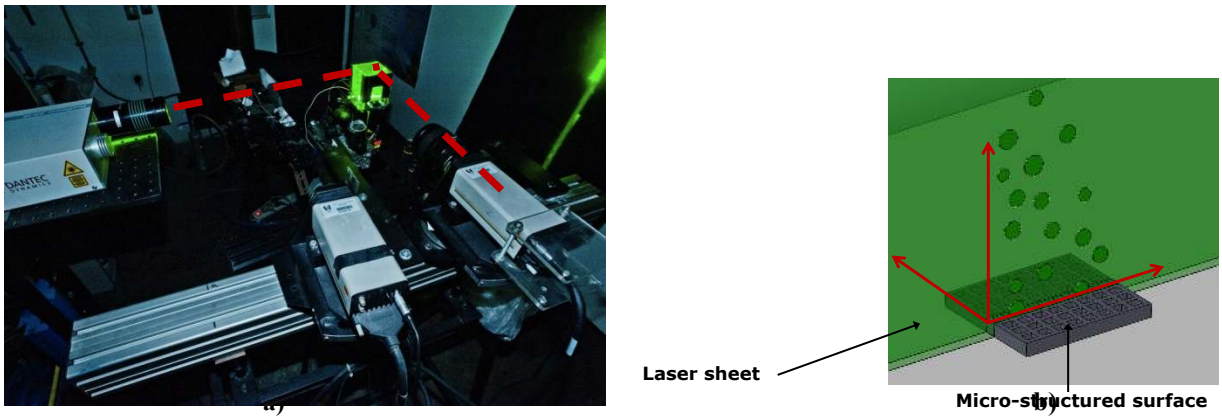

Figure 2 a) PIV arrangement and **b)** coordinate system considered for the PIV measurements.

RESULTS AND DISCUSSION

A detailed analysis of bubble dynamics concerning the quantitative evaluation of the bubble departure diameter and frequency as well as nucleation sites density is performed for water, ethanol and HFE7000 over the same surfaces studied here, in a previous work [10]. Based on a force balance to the bubble at detachment it is clear that the largest bubbles are formed during the boiling of the fluid with the largest surface tension (water). The departure frequency is similar for most of the surfaces, for the three liquids, but there is a significant reduction of the frequency of the water bubbles, for the surface with the smallest *S*, which is associated to an excessively promoted coalescence.

The relation between coalescence and the distance between the cavities is easily confirmed in Figure 3: the coalescence factor $D_b/D >> 1$ (being D_b the averaged bubble diameter and D the diameter as the bubble exits the cavity, i.e. with no coalescence) for water and varies significantly with *S*, thus evidencing the strong coalescence effects observed at water boiling (Figure 3a). This behaviour contrasts with that of well wetting fluids, with low surface tension, such as ethanol and HFE7000 (Figures 3b and 3c, respectively).

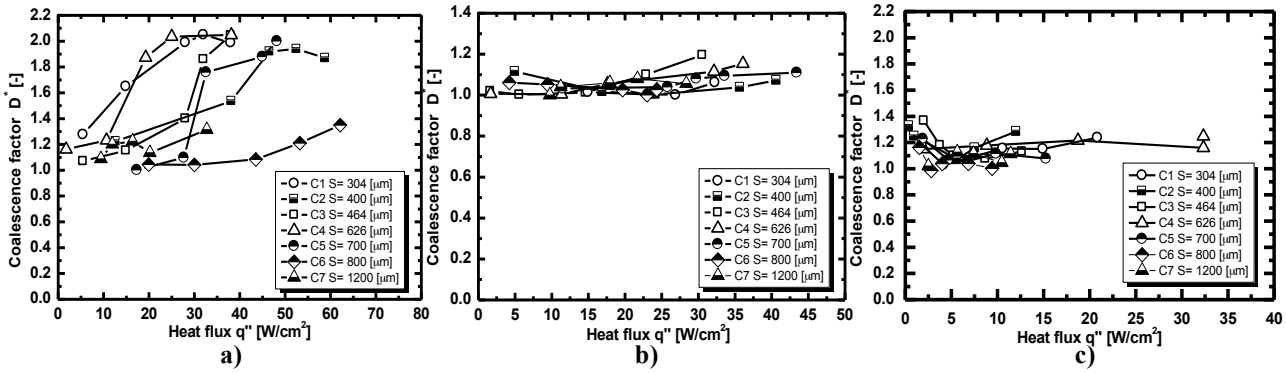

Figure 3 Coalescence factor versus heat flux for pool boiling over micro-patterned surfaces for: a) water, b) ethanol, c) HFE 7000.

This analysis is consistent with the boiling curves and heat transfer coefficients shown in Figure 4: although ethanol and HFE 7000 presented a more homogenous and vigorous boiling with limited interaction mechanisms (and particularly coalescence), this was not enough for these fluids to reach the overall higher heat transfer coefficients of water. Nevertheless, the strong horizontal coalescence phenomena characterizing water boiling on surface C1 (S=304 μm), leads to a steep deterioration of the heat transfer coefficient, so that the heat transfer of water and ethanol are quite similar for the aforementioned surface. Hence, the coalescence effects can be empirically related to the distance *S* since this distance between cavities is directly acting on the coalescence mechanisms which occur close to the surface and so should be well related to the force balance describing the bubble detachment, as proposed by Fritz [11] and followed by many other researchers to scale bubble departure diameters: $Lc=(\sigma_{lv}/(\rho_l-\rho_v))^{1/2}$. This empirical relation, earlier suggested in [4] is extended here for ethanol and HFE7100 pool boiling in Figure 5.

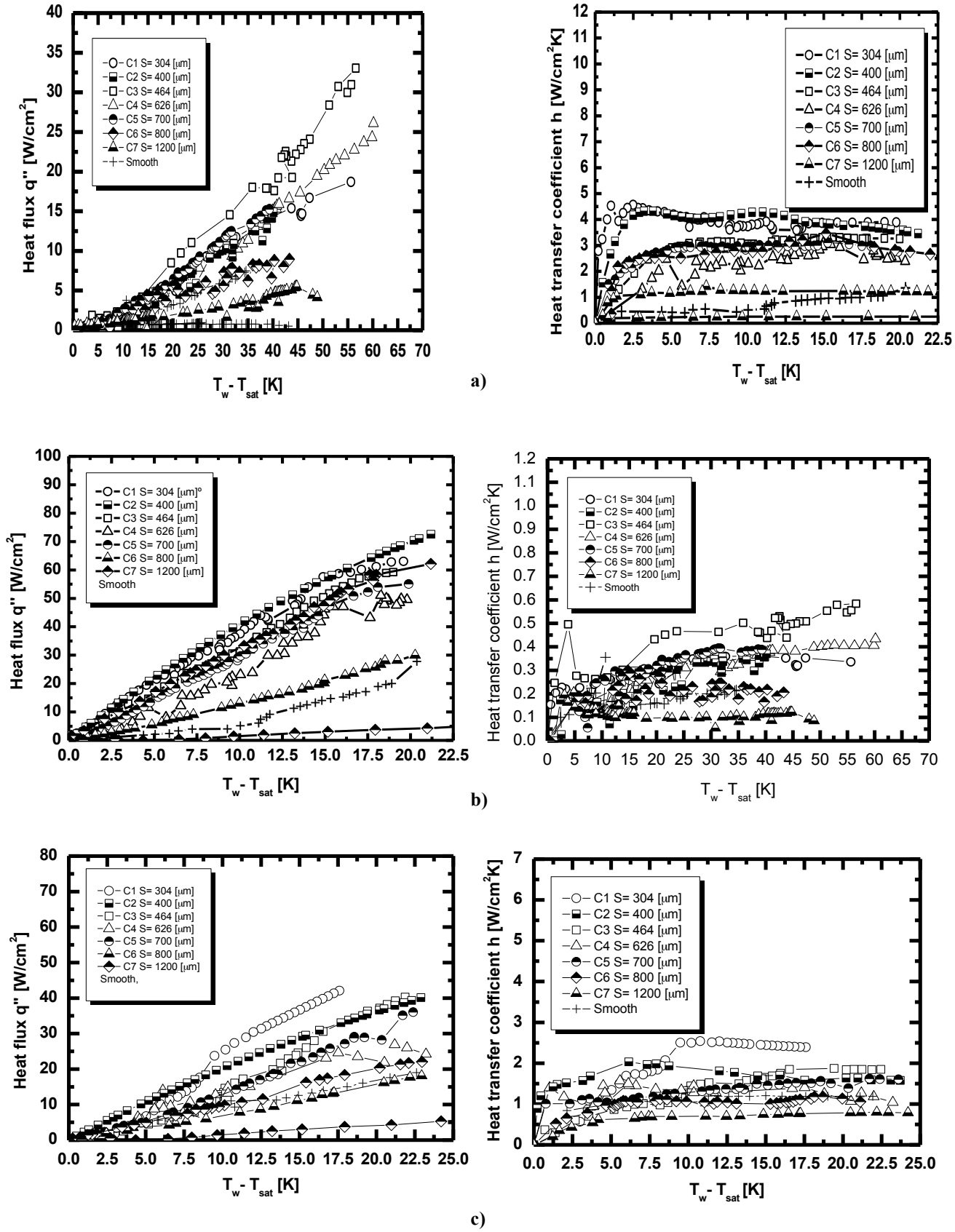

Figure 4 Boiling curves and heat transfer coefficients over micro-patterned surfaces of a) water, b) ethanol, c) HFE7000.

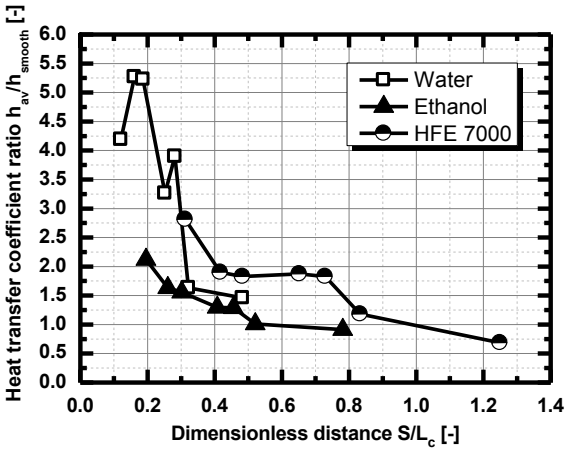

Figure 5 Heat transfer ratio vs dimensionless distance for water, ethanol and HFE 7000 in the range of patterns studied.

The representation in Figure 5, already allows to account for the relative improvement of the performances using the micro-patterned surfaces since, on one hand compares the enhancement of the heat transfer coefficient (given by the three heat transfer parcels: natural convection, evaporation and induced bulk convection) using each micro-textured surface in relation to that of the smooth surface. On the other hand, the distance *S* is related to the characteristic bubble departure dimensions. This relation is important as it defines the critical distance *S* up to which the bubbles with a certain diameter, depending on the balance between surface tension and buoyancy forces ($Lc=(\sigma_{lv}/(\rho_l-\rho_v))^{1/2}$) will coalesce. Such relation must still be refined, but one may already identify a maximum for the water boiling, which is related to the maximum *S* above which the horizontal coalescence will conduce to the declination of the heat transfer coefficient (as identified in the boiling curves in Figure 5).

The absolute values of h, being the result of the sum of the 3 parcels of the heat transfer [5] are dominated by the largest values of the thermal properties of the water, which presents the highest values of h, despite its worse performance as *S* decreases. However, the plot in Figure 5 clearly indicates that although the properties of ethanol, namely the latent heat of evaporation are significantly larger than those of HFE7000, the relative enhancement in the heat transfer obtained with the micro-patterned surfaces is higher than that obtained for ethanol, so the curve for HFE7000 is actually above that of ethanol. This is probably due to significant improvement of the micro-structure on bubble dynamics, which is affecting one of the parcels of the total heat transfer. Given the low thermal properties of HFE7100, the most probable effect of *S* should be on the induced bulk convection. To infer on this, a detailed study of bubble dynamics was performed, based on PIV measurements.

FLOW DESCRIPTION: ANALYSIS OF THE AVERAGE VERTICAL BUBBLE VELOCITY

The effect of the surface patterning in the parcel of the induced convection was investigated evaluating the average vertical bubble velocity (average of the velocity profile for a fixed value of H/D), along the vertical dimensionless distance H/D, where H is the vertical distance from the top face of the surface in (mm) and D is the bubble departure diameter (also in mm), for different heating conditions and different micro-patterns. Naturally that this effect is relevant close to the surface, but given the well known restrictions of PIV measurements performed very close to the surface (*e.g.* Raffel *et al.* [12]) the assessment of bubbles' velocity must be performed at various distances H/D, in order to understand bubbles´ motion. The results are presented in Figure 6, for ethanol and HFE7000, boiling over micro-patterned surfaces with decreasing *S*.

Overall, the bubbles are ejected with larger average velocity, as the imposed heat flux is higher, although this trend is more evident for ethanol. The bubbles then decelerate due to the braking effect forced by the zero velocity at the top of the pool. This is quite more evident in ethanol pool boiling with is related to its physico-chemical properties and to a less efficient boiling process, as aforementioned. Indeed a vigorous boiling activity already pointed out for HFE7000 can be identified in the analysis of the bubbles vertical velocity profiles. There is a strong oscillation along the vertical velocity around the mean value for HFE7000, which is speculated to be due to the very vigorous boiling. Similarly to what is observed for ethanol, surfaces with closer cavities (C2 S=400μm, and C5 S=700μm) present more uniform and stable profile when compared to those with sparser cavities (C6 S=800μm, and C7 S=1200μm). In fact it is now clearer that the stronger interaction phenomena still occur at the surface with closer cavities, but they are observed at a higher distance from the wall for HFE7000, when compared to ethanol and to water. Hence, the coalescence will still affect directly the heat transfer of ethanol by producing vapor bubbles which block the fluid circulation near the surface, while

for HFE7000 it contributes for the formation of a denser bubble plume, acting as stabilization factor when one speaks in terms of vertical velocities.

For surfaces with sparser cavities, the oscillations of the vertical velocity are more evident than those observed for ethanol, due to the higher number of active nucleation sites and the higher value of bubble departure frequency. However, the vertical velocity is overall much higher for HFE7000, so at the end, the induced bulk convection is more efficient for this liquid, when compared with ethanol.

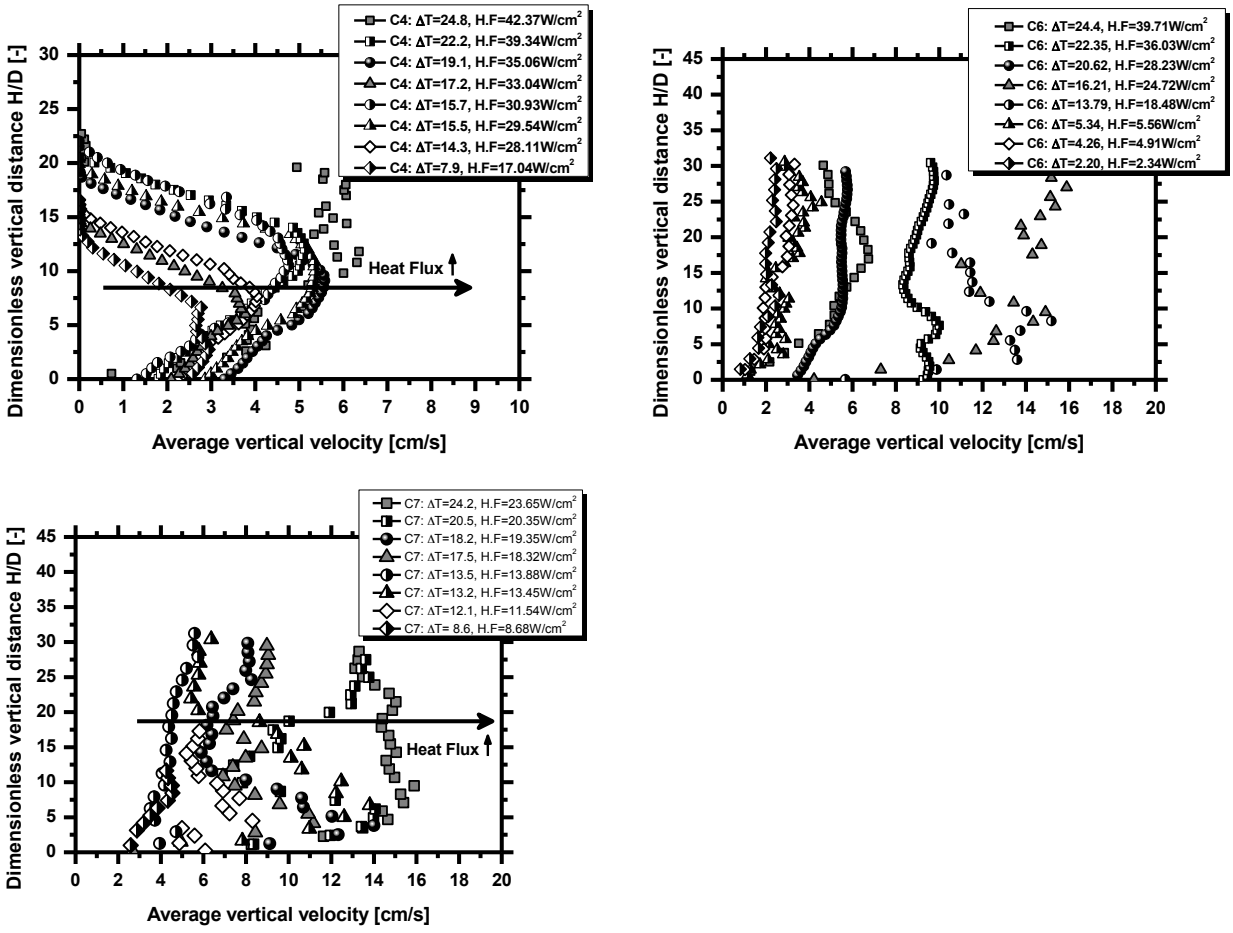

a)

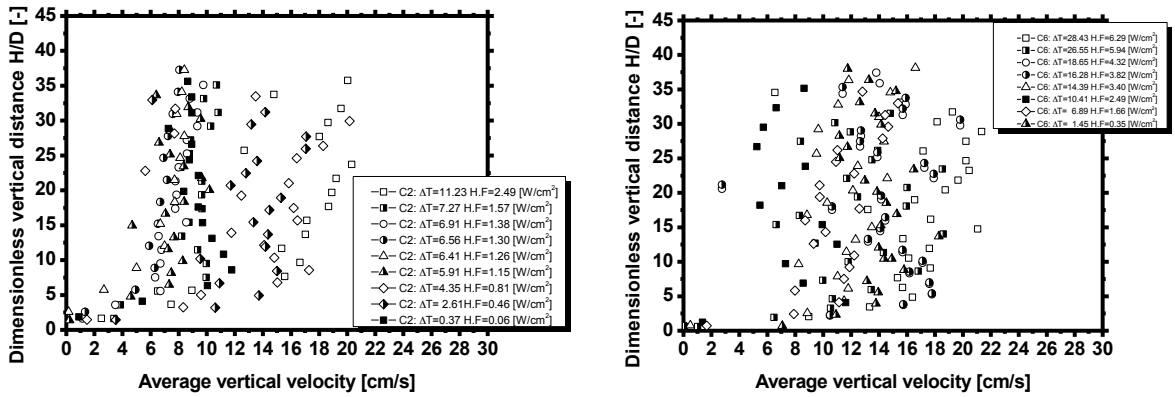

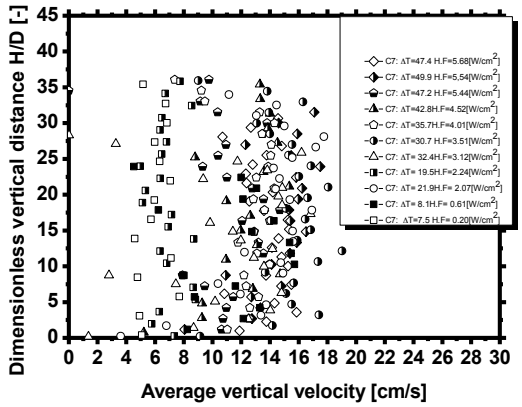

b)

Figure 6 Vertical velocity profile for a) Ethanol and b) HFE 7000 over micro-patterned surfaces: C2 S= 400 μm, C6 S= 800 μm and C7 S= 1200 μm.

The much higher bubble vertical velocities measured for HFE7000 when compared to that of ethanol are quite evident in Figure 7. The overall value oh h is yet larger for ethanol, as it results from the sum of the 3 heat transfer parcels.

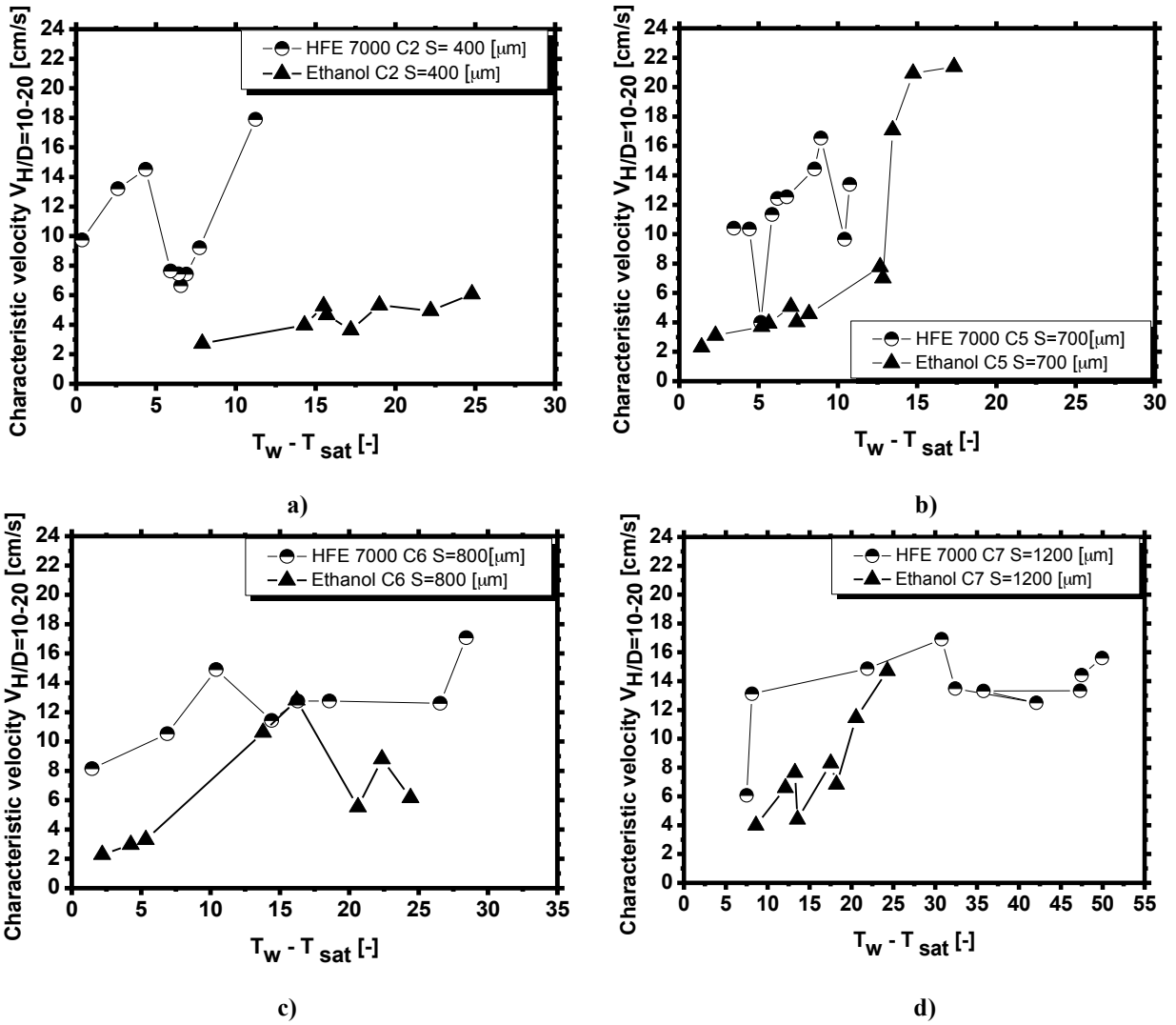

Figure 7 Characteristic velocity vs wall superheat for ethanol and HFE 7000. a) Surface C2 (S=400 μm) b) Surface (C5 S=700 μm c) Surface (C6 S=800 μm) d) Surface (C7 S=1200 μm).

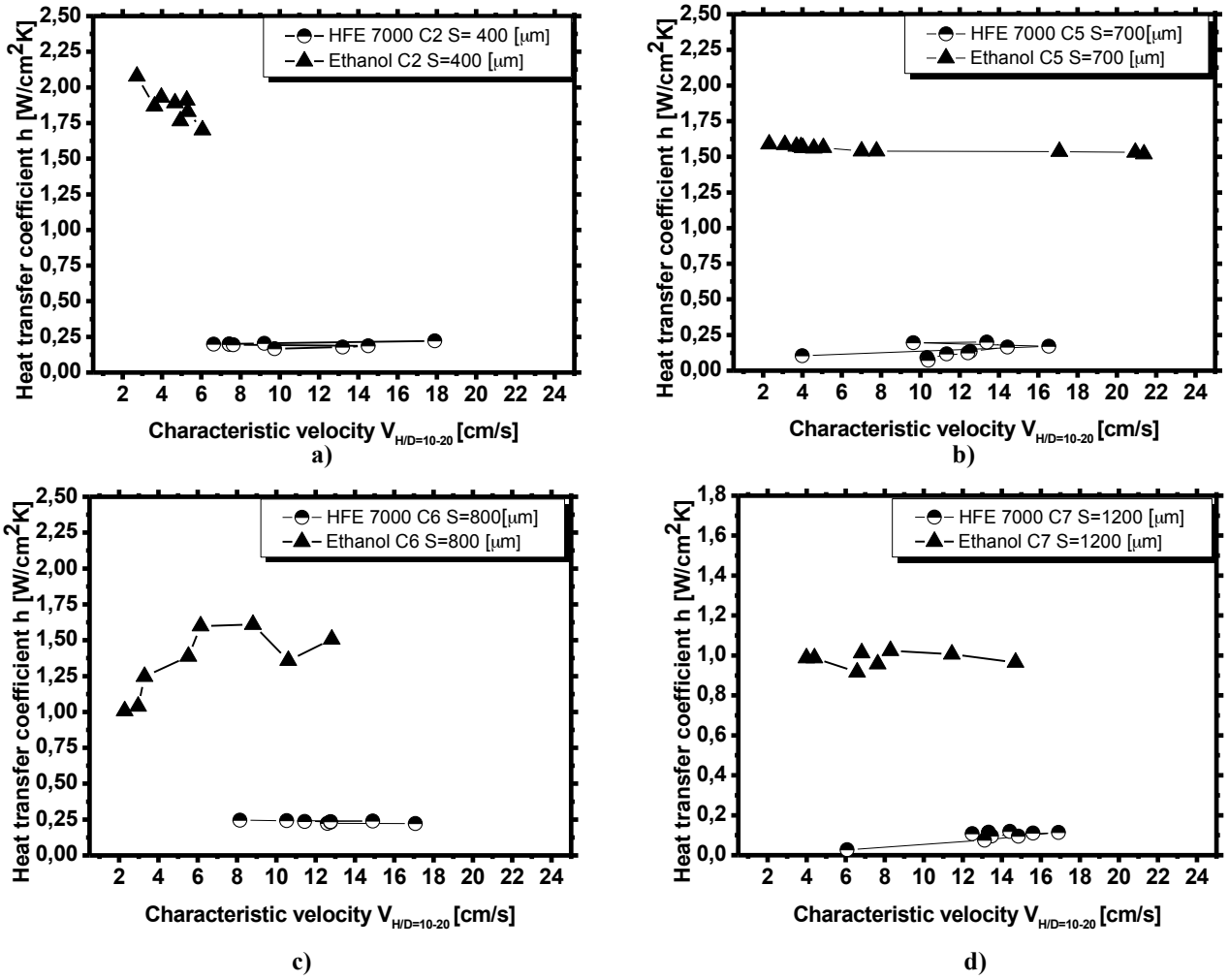

Figure 8 Heat transfer coefficient versus characteristic velocity for ethanol and HFE 7000. a) Surface C2 (S=400 μm), b) Surface C5 (S=700 μm), c) Surface C6 (S=800 μm), d) Surface C7 (S=1200 μm).

This analysis is consistent if the parcel of the induced bulk convection is more important, relatively to the others, which is true, if one considers the approach of other researchers such as Kandlikar [3] or Gerardi *et al.* [13,14]. Indeed, considering that the induced bulk convection is strongly related to the so-called quenching heat flux, which is proportional to $f_b.N_{SD}$ (being f_b the bubble frequency N_{SD} the active nucleation sites density), it is clear the importance of augmenting these two parameters, as achieved in the HFE7000 with the micro-patterned surfaces. This parcel of bulk induced convection is actually estimated in our study to be dominating, which is in agreement with the observations of Gerardi *et al.* [13,14]. The approach followed here allows to obtain experimentally all the data that is required to check on the universality of the formulations devised by many of these authors (*e.g.* [3, 13, 14]). However, these formulations are rather empirical so that a more theoretical approach is preferred, possibly based on the classical relation $Nusselt=Reynolds^{a}Prandtl^{b}$, which should be compared to some empirical approaches in the near future.

SUMMARY

The present work introduces an alternative approach which combines heat transfer measurements, high speed visualization and PIV to infer on the effect of surface micro-structuring in the various heat transfer parcels.

The results confirm the importance of enhancing the pool boiling performance, by promoting the increase of the bubble frequency and active nucleation sites density with micro-patterned surfaces. The role of the patterns is different, depending on the properties of the fluids. Hence, for liquids with very high latent heat of evaporation and surface tension, the parcel of heat transfer related to the phase change is very important. Based on the force balance on the departing bubbles, it is evident that in this case the micro-patterns will mainly affect the bubble coalescence, which may

lead to steep deterioration of the heat transfer coefficient. On the other hand, for liquids with lower thermal properties (and lower surface tension) the micro-patterns play an important role in increasing and stabilizing the vertical velocity of the bubbles, thus favoring a very efficient boiling performance, with high boiling frequencies and high active nucleation sites density. This role of the micro-patterned surfaces is well captured by the representation proposed here, which relates the heat transfer coefficient with the distance between micro-patterns *S*, made dimensionless by the characteristic dimension ($Lc=(\sigma_{lv}/(\rho_l-\rho_v))^{1/2}$). This representation actually shows the best performance of the HFE7000 in comparison to that of ethanol, when the micro-patterned surfaces are used, despite the lower thermal properties of HFE7000. This trend was confirmed experimentally in our measurements.

ACKNOWLEDGMENTS

The authors are grateful to Fundação para a Ciência e a Tecnologia (FCT) for partially financing the research under the framework of project PTDC/EME-MFE/109933/2009 and for supporting A.S. Moita with a Fellowship (Ref.:SFRH/BPD/63788/2009).

REFERENCES

[1] Chu K-H, Enright R and Wang EN "Structured surfaces for enhance pool boiling heat transfer" Appl. Phys. Lett. 100 (2012) 241603.

[2] McHale JP and Garimella SV "Bubble nucleation characteristics in pool boiling of wetting liquid on smooth and rough surfaces" Int. J. Multiphase Flow 35(2010) pp.249-260.

[3] Kandlikar SG "A theoretical model to predict pool boiling CHF incorporating effects of contact angle and orientation" J. Heat Transf.

[4] Moita AS, Teodori E, Moreira ALN "Enhancement of pool boiling heat transfer by surface micro-structuring" Journal of Physics: Conf. Series 935 (2012) 012175 (doi: 10.1088/1742-6596/395/1/012175)

[5] Han CY and Griffith P "The mechanism of heat transfer in nucleate boiling" Technical Report No 7673-19, Dep. Mech. Eng. MIT, USA (1992).

[6] Moita AS, Moreira ALN "Scaling the effects of surface topography in the secondary atomization resulting from droplet/wall interactions" Exp. Fluids, 52:3(2012) pp.679-695.

[7] Bostanci H. "Thermal Challenges in Next Generation Electronic Systems" Joshi & Garimella (Eds), Millpress, Rotterdam, ISBN 90-77017-03-8 (2002).

[8] Sasaki T., Nagai N., Murai Y., Yamamoto M., "Particle Image Velocimetry measurement of bubbly flow induced by alkaline water electrolysis" In: Proc. of PSFVIP-4, Chamonix, France (2003).

[9] Cheng W., Murai Y., Sasaki T., Yamamoto M. "Bubble velocity measurement with a recursive cross correlation PIV technique" Flow Meas. Instr 16(2005) pp.35-46.

[10] Teodori E., Moita AS, Moreira ALN, "Pool boiling heat transfer over micro-patterned surfaces: experiments and theory", to be presented at the 8th World Conf. Exp Heat Transf., Fluid Mech. and Thermodynamics, ExHFT-8, Lisbon, Portugal, 2013.

[11] Fritz W., "Maximum Volume of Vapor Bubbles" Phys Z.36(1935) pp. 279-385.

[12] Raffel M., Willert C., Wereley S., Kompenhans, J. Particle Image Velocimetry: a practical guide. 2nd Ed., Springer Verlag, Heidelberg (2007).

[13] Gerardi C., Buongiorno J., Hu L-w., McKrell T., "Study of bubble growth in water pool boiling through synchronized, infrared thermometry and high-speed video", Int. J. Heat Mass Transf, 53(2020) pp.4185-4192.

[14] Gerardi C., Buongiorno J., Hu L-w., McKrell T., "Infrared thermometry study of nanofluids pool boiling phenomena", Nanoscale Res. Lett., 6(2011):232